Stabilisation of the swing pattern of an anisotropic simple pendulum

OPEN ACCESS
IOP Publishing
European Journal of Physics
Eur. J. Phys. **45** (2024) 055003 (12pp)
https://doi.org/10.1088/1361-6404/ad6362

Stabilisation of the swing pattern of an anisotropic simple pendulum

E McGlynn[1,2], C Saracut[1] and A A Cafolla[1,3]

[1] School of Physical Sciences, Dublin City University, Glasnevin, Dublin 9, Ireland
[2] National Centre for Plasma Science and Technology, Dublin City University, Glasnevin, Dublin 9, Ireland
[3] National Centre for Sensor Research, Dublin City University, Glasnevin, Dublin 9, Ireland

E-mail: enda.mcglynn@dcu.i.e

Received 25 April 2024, revised 25 June 2024
Accepted for publication 15 July 2024
Published 2 August 2024

Abstract

The suppression of the effects of anisotropy on a pendulum by use of a rotating mount was initially envisaged by Léon Foucault, based on his observations of the vibrations of a rod clamped in a lathe. However, the method seems to never have been tried due to the practical difficulties involved. We report a computational study of the stabilisation of the swing pattern of a simple pendulum, showing anisotropic behaviour in a static configuration, by rotation of the system mount. When the mount is static, for most initial conditions the swing patterns quickly evolves into unstable, complex Lissajous-like patterns. When the pendulum mount is rotated faster than the pendulum frequency effects of anisotropy are suppressed, and the swing pattern stabilises to that of an isotropic 3D simple pendulum. Suppression of mount anisotropy influence occurs for relatively low rotation rates. We also study swing evolution in the presence of random variations in the orientation of the mount principal axes. The use of computational techniques confirms Foucault's original observations and hypothesis and provides an interesting avenue for students to engage meaningfully with this historically important and inspiring experiment in a novel and challenging manner.

Supplementary material for this article is available online

Keywords: swing, anisotropic, simple, pendulums, Foucault, stabilisation

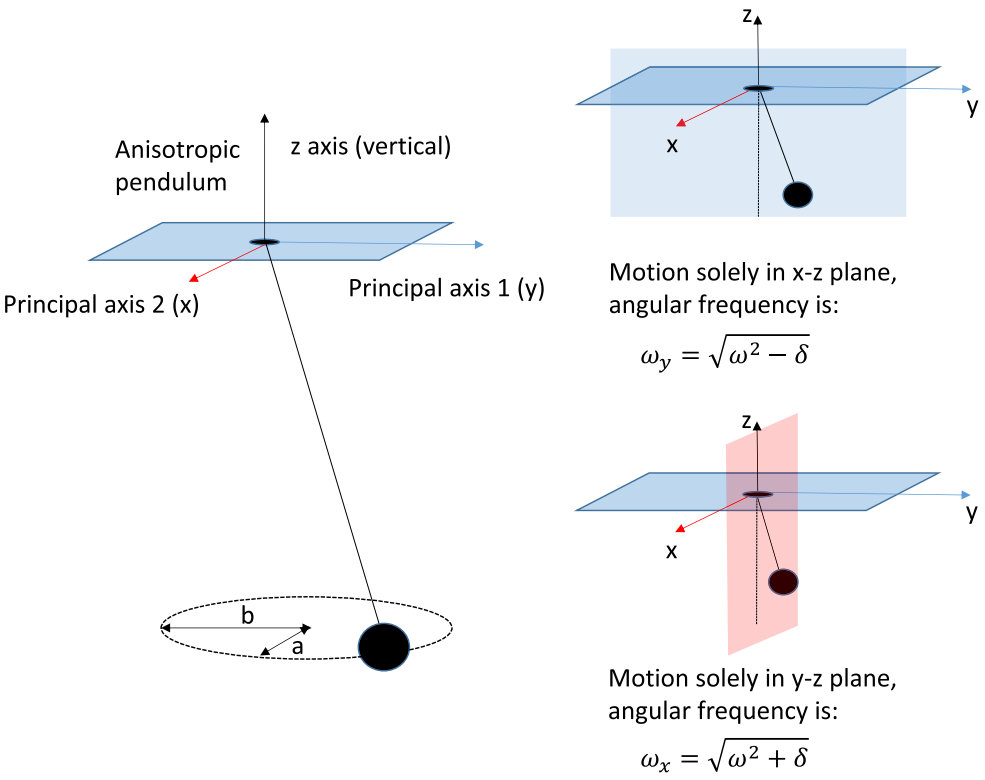

Figure 1. Schematic diagram of simple pendulum with anisotropy. The principal axes (PA) are shown and the associated natural oscillation frequencies are also indicated.

1. Introduction

The simple pendulum is a mainstay of undergraduate courses in classical mechanics, and it displays a range of interesting physics beyond the most basic, simple harmonic oscillator (SHO), example [1]. One of the most famous examples of the use of a simple pendulum is the Foucault pendulum [2]. In practice the construction of a Foucault pendulum which displays the idealised behaviour and facilitates a demonstration of the earth's rotation is a significant challenge due to damping of the motion, the natural precession associated with a non-planar swing and the anisotropy of the pendulum system. Foucault himself was well aware of all three of these issues and conducted various studies concerning these aspects [3].

The main focus of the present report is the practically unavoidable anisotropy of the pendulum system, which means that the pendulum essentially has two orthogonal principal axes (PA), with slightly different natural oscillation frequencies associated with planar swing motions along the two PA, as shown schematically in figure 1 below [4]. As is well known, any initial condition which has components of displacement or velocity along both the PAs will lead to a time-varying and complex Lissajous-like pattern where the initial elliptical shape distorts as its major and minor axes change in size. This completely masks the relatively small precessions associated with the rotation of the earth and those due to the natural precession. While in principle launching the pendulum such that its motion is confined to a single PA direction should eliminate this problem, in practice this is essentially impossible.

There is quite a body of literature on methods to reduce anisotropy in the pendulum system [5–7], including from Heike Kamerlingh Onnes [8].

The classical methods involve (i) a very long pendulum wire and a heavy bob, to ensure small angle motion, small anisotropy and minimal effects of air damping and (ii) a careful launch to ensure close to planar motion. However physically smaller systems face considerable difficulties, including anisotropy, and an experienced observer and builder of such systems, H R Crane, notes that '*Making the mechanical system more perfect only slows the growth; it does not prevent it from reaching an intolerable magnitude eventually*', in relation to the growth of the minor axis of the elliptical motion, a view also shared by more recent authors [9, 10].

It is interesting to note that Foucault himself proposed a very novel, if difficult to implement, potential solution to this problem. The inspiration seems to have come from his observations of the behaviour of the vibrations of a rod clamped in a lathe. This system seems to have been a rich vein for Foucault since it also inspired his original thoughts concerning the behaviour of his eponymous pendulum as the earth rotates [11]. In his biography of Foucault, William Tobin mentions comments Foucault addressed to the Société Philomathique, as follows: '*Whatever the rod's vibration…it was frozen in this path and ceased to evolve when he turned the chuck at more than a couple of revolutions per second.*' [3] Tobin further comments that this was hardly a practical proposition, and that Foucault never seems to have tried this approach in practice. Further evidence supporting the effectiveness in practice of an approach whereby the mount of the oscillating system is rotated can be found in [9] of the paper of Tobin and Pippard [2], who note that for the case of a vibrating rod in a lathe that '*If the rod is insufficiently isotropic there will be two (perpendicular) directions only in which the rod will vibrate in a plane; set vibrating at other angles, with the chuck at rest, the rod will ellipse.*' This may be read to imply that if the chuck rotates the rod will not ellipse ('ellipse' here meaning the distortion of the initial vibration pattern by the growth of the minor axis of the elliptical motion[4]), though this is not elaborated further.

However, this interesting proposition is readily studied using a computational approach, using tools and techniques familiar to advanced undergraduate students, and could be used as an open-ended assignment in a computational physics module. It is an example of a physical system which is too complex to solve analytically due to the time variation of the pendulum mounting orientation, but which is relatively easily solved numerically, using either a 'home-made' 4th order Runge–Kutta solver, or one of the differential equation solvers available in Python (the latter being considerably faster). As such it is an interesting example for undergraduate students to explore and offers possibilities for interrelated computational and experimental project work as well as for more open-ended studies, some examples of which are suggested. These final points are relevant to a recent article by Flannery in the American Journal of Physics [13].

The importance of this topic and its particular interest to students studying physics lies mainly in two domains. Firstly, as mentioned above, the simple pendulum is a mainstay of undergraduate courses in classical mechanics, and it displays a range of interesting physics beyond the most basic, SHO, behaviour. Pendulum and oscillator systems beyond the basic SHO are important in a range of applications, including laser physics, nonlinear dynamics and electronics (e.g. the van der Pol oscillator, Chua diode and memristor circuitry) [14–17]. Furthermore, this example illustrates the effects of a changing environment on a physical system, which is of relevance in a variety of areas of advanced physics. For example, in

[4] The term 'ellipsing' is occasionally used in the literature to mean the precession of the vertices of the elliptical trajectory of the pendulum [12], differently to the usage of Tobin and Pippard [2] and of this work.

nuclear magnetic resonance (NMR) systems it is regularly observed that the seemingly more chaotic environment of a liquid leads to narrower NMR spectral lines than the less chaotic solid crystal environment (in the absence of 'magic-angle' spinning) [18], due to motional narrowing of the NMR lines [18–20]. In addition, the stabilisation of particle and system motions in unstable potentials via time variation of system parameters (including rotation) has been reported in a variety of physical systems [21–25]. Hence introducing students to pendulum and oscillator systems beyond the SHO classroom example, and to computational methods and tools which can be used to study such systems, is an excellent way to prepare students for these more advanced areas of physics and associated application areas.

2. Summary of mathematical and computational details

Details of the mathematical background and computational approach are provided in the supplemental material accompanying this article. Only a knowledge of Newtonian mechanics at the undergraduate level is required, and for the sake of brevity we provide only a summary here. To represent the pendulum motion in 2D beyond the linear approximation we modify the results of the analysis of Olsson [26]. For the x- and y-components in an anisotropic system the modified equations are (with some corrections of small typographical errors in Olsson's work, as discussed in the supplementary material):

$$a_x = -\omega_x^2 x\left(\sqrt{1-\frac{(x^2+y^2)}{l^2}}\right) - \left(\frac{x}{l^2}\{v_x^2+v_y^2\}\right) - \left(\frac{x}{l^4}\left[\{xv_x+yv_y\}^2 \Big/ \left\{1-\frac{(x^2+y^2)}{l^2}\right\}\right]\right) \tag{1a}$$

$$a_y = -\omega_y^2 y\left(\sqrt{1-\frac{(x^2+y^2)}{l^2}}\right) - \left(\frac{y}{l^2}\{v_x^2+v_y^2\}\right) - \left(\frac{y}{l^4}\left[\{xv_x+yv_y\}^2 \Big/ \left\{1-\frac{(x^2+y^2)}{l^2}\right\}\right]\right). \tag{1b}$$

The simplest way to incorporate anisotropy in the system is to modify Olsson's original equations to replace ω with ω_x and ω_y, the angular frequencies associated with the two orthogonal PA, i.e. ω_x and ω_y, respectively, as shown in equations (1a). The details of the equations are discussed in the supplemental material. A schematic diagram of the modelled configuration is shown in figure 1.

We believe this approach appropriately captures the essential physics of the situation by absorbing the various possible sources of system anisotropy into the parameters ω_x and ω_y. The anisotropy of the system is described following Pippard's approach [4], and is parametrised by the quantity δ, assuming the anisotropy is relatively small, and defining $\omega_x^2 = \omega^2 + \delta$ and $\omega_y^2 = \omega^2 - \delta$, where ω^2 is the mean of the squared frequencies for pendulum motion along the two PA directions.

The crux of the computational approach is to utilise the PA frame solely for the calculation of the acceleration components using equations (1a), since the calculation of the acceleration is especially simple in the PA frame. At any instant in time the coordinates of the position and velocity vectors in the inertial laboratory frame are known, and then transformed by rotations into the PA frame. The $_{ax}$ and a_y components of the acceleration vector are then calculated

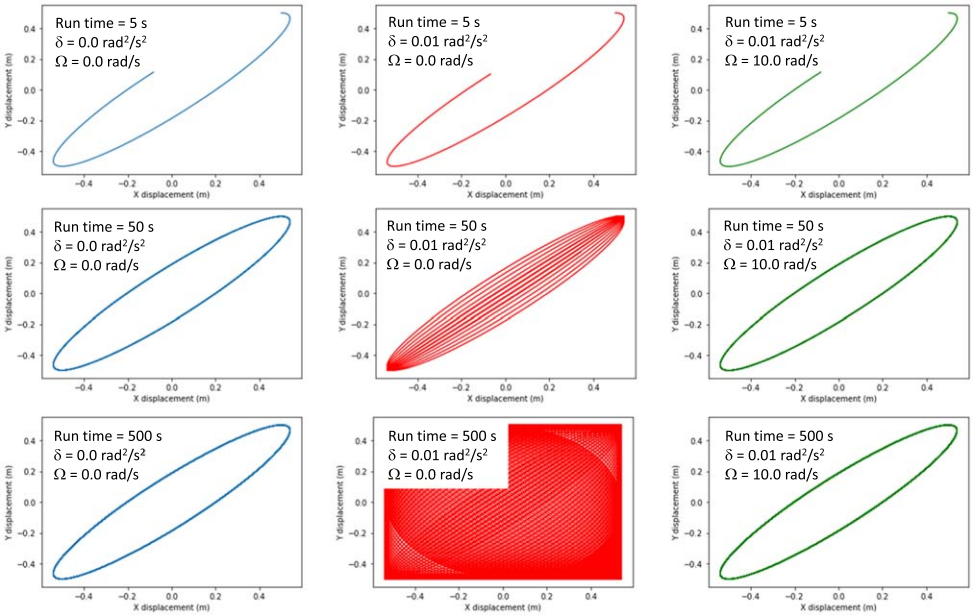

Figure 2. Trajectories of 2D pendulum (x displacement versus y displacement) in linear regime calculated using odeint. Left panel shows isotropic pendulum ($\delta = 0\,\mathrm{rad}^2/\mathrm{s}^2$) with stationary mount ($\Omega = 0\,\mathrm{rad\,s}^{-1}$) at times 5 s (top), 50 s (middle) and 500 s (bottom). The middle panel shows an anisotropic pendulum ($\delta = 0.01\,\mathrm{rad}^2/\mathrm{s}^2$) with stationary mount ($\Omega = 0\,\mathrm{rad\,s}^{-1}$) at times 5 s (top), 50 s (middle) and 500 s (bottom). The right panel shows an anisotropic pendulum ($\delta = 0.01\,\mathrm{rad}^2/\mathrm{s}^2$) with rotating mount ($\Omega = 10\,\mathrm{rad\,s}^{-1}$) at times 5 s (top), 50 s (middle) and 500 s (bottom). For all these calculations the pendulum length was set to 10 m, with initial conditions of $x = 0.5$ m, $v_x = 0.2\,\mathrm{m\,s}^{-1}$, $y = 0.5$ m, and $v_y = 0.0\,\mathrm{m\,s}^{-1}$.

using equations (1a), and these are transformed back into the inertial laboratory frame, and then used in the computational differential equation solver to increment the motion and calculate the new position and velocity vectors in the laboratory frame. These acceleration (and other vector) components in the laboratory frame are then used in the differential equation solver. At each time, t, the angular rotation of the PA frame relative to the laboratory is calculated using $\theta = \Omega.t$, where Ω is the angular velocity of rotation of the system (see figure SI-1 in the supplemental information).

The full code used for both the linear and nonlinear regimes, with comments, is provided in the supplemental material. In our initial approach to the problem we utilised a simple 4th order Runge–Kutta (RK4) approach, which was programmed *ab initio* and this was compared to existing Python functions to check the accuracy of the solutions. A number of initial checks were made of the code, as described in the supplemental information, in particular figure SI-2.

3. Results and analysis

3.1. Linear regime

For the case of the linear regime described by equations (SM1) in the supplemental material, one can see in the left-hand panel of figure 2 the evolution of the motion of an isotropic

pendulum system whose initial conditions lead to a closed elliptical orbit over a number of time intervals (the details of the pendulum and relevant simulation parameters are provided in the caption). The middle panel of figure 2 shows the evolution of the motion of this pendulum when an anisotropy of $\sim$1% (compared to the value of ω^2; $\omega^2 \approx 1\,\mathrm{rad}^2/\mathrm{s}^2$ and $\delta \approx 0.01\,\mathrm{rad}^2/\mathrm{s}^2$) is introduced, with the mount remaining stationary. The evolution in this case shows a clear and growing distortion of the initial elliptical shape as the major and minor axes change in size, and a very complex pattern of motion ensues, of the type referred to by Crane and Schulz-Dubois [8, 9]. The right-hand panel shows the evolution of the motion of this same anisotropic pendulum when the mount is rotated at an angular velocity (Ω) equal to approximately ten times that of the mean pendulum swing angular frequency in the PA frame, ω. It is immediately clear that the closed elliptical orbit pattern seen for the isotropic pendulum is recovered and that the growing distortion of the initial elliptical shape seen in the middle panel is no longer observed. The evolution is shown in more detail in the supplemental material, figures SI-3 and SI-4, where additional panels show (i) the transition from the left panel to the middle panel of figure 2 (with $\delta = 0.005\ \mathrm{rad}^2/\mathrm{s}^2$; figure SI-3) and (ii) the transition from the middle panel to the right panel (with $\Omega = 5\,\mathrm{rad\,s}^{-1}$; figure SI-4).

Figure 3 shows a comparison of the oscillations of the x- and y-axis components over time (from 450 to 500 s after launch) for the case of the isotopic system, stationary anisotropic system (the x- and y-axes coincide with the PA of mount), and rotating anisotropic system, with identical parameters to those in figure 2. It is seen clearly that the oscillation frequency of the rotating anisotropic pendulum matches that of the isotropic pendulum to a high degree of accuracy over an extended time period (close to 500 s) and is clearly different to the two oscillation frequencies seen for the stationary anisotropic pendulum. Data from 0 to 100 s, and from 450 to 500 s after launch are shown in the supplemental material, figure SI-5, to allow comparison of the behaviour at shorter and longer delays after starting the motion. Figure SI-6 shows the differences between the calculated x- and y- components over time of the isotopic system and rotating anisotropic system presented in figure 3 and SI-5; small differences (at the level of $\sim$0.1%) in the two solutions are evident, which show periodicity at both the average oscillation frequency and at twice the mount rotation frequency as expected. Note that the effective rotation frequency of the mount is actually 2Ω, i.e. when the PA rotate through π radians the same physical situation is obtained as for a rotation angle of zero (it is only the orientation of the axes, not the positive and negative axis directions, which affects the motion).

3.2. Nonlinear regime

For the nonlinear regime described by equations (1a), we show in figure 4 results for the case of the isotopic system, stationary anisotropic system (the x- and y-axes coincide with the PA of mount), and rotating anisotropic system in the left-hand, middle and right-hand panels, respectively, over a number of time intervals (the details of the pendulum parameters are provided in the caption). The pendulum length and initial conditions are the same as for the data in the linear regime in figure 2 and are chosen to allow comparison with the analytical result for the natural precession which arises from an analytical solution of Olsson's isotropic approximate equations shown in the supplemental material (SM2).

The evolution of motion in the case of the isotropic system now clearly shows evidence of an elliptical motion with this natural precession, which is shown in the supplemental material to equal the theoretically expected value of $3\omega(ab)/8l^2$, as mentioned below. The motion of the stationary anisotropic system shows a much more complex evolution, again with a clear and growing distortion of the initial motion shape which renders it impossible to recognise or

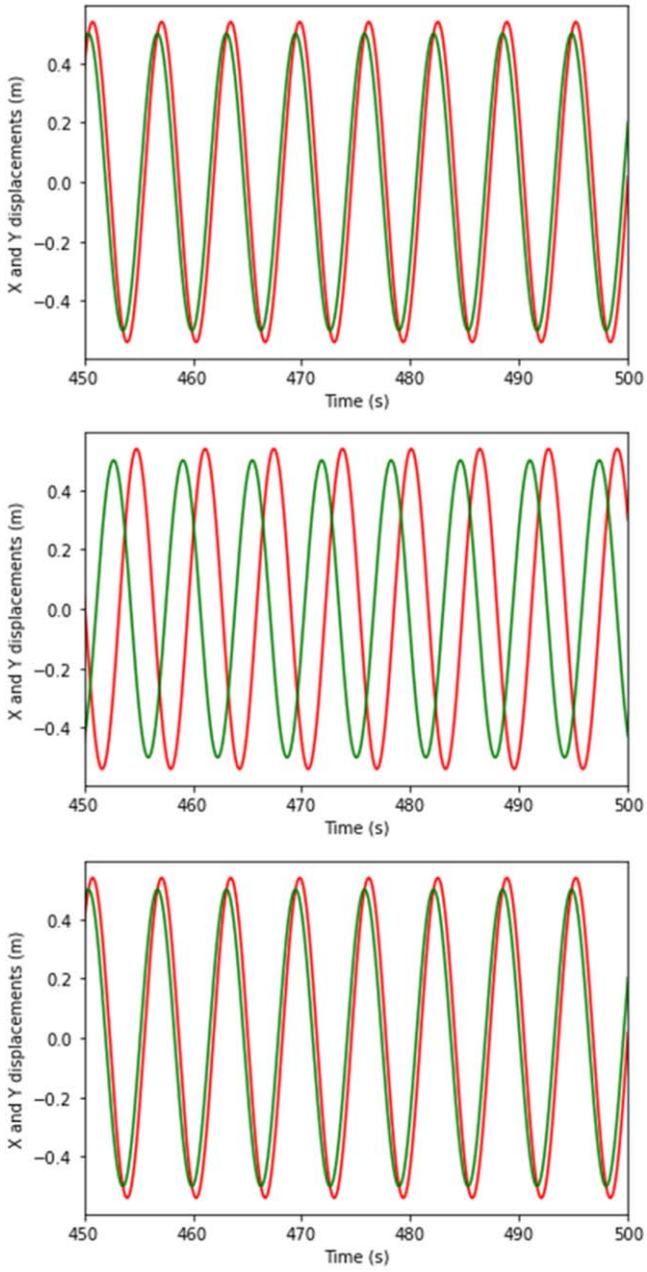

Figure 3. X displacement in red and Y displacement in green, versus time, of 2D pendulum from 450 to 500 s) in linear regime calculated using odeint. Top panel shows isotropic pendulum ($\delta = 0\,\mathrm{rad}^2/\mathrm{s}^2$) with stationary mount ($\Omega = 0\,\mathrm{rad\,s}^{-1}$), middle panel shows anisotropic pendulum ($\delta = 0.01\,\mathrm{rad}^2/\mathrm{s}^2$) with stationary mount ($\Omega = 0\,\mathrm{rad\,s}^{-1}$) and bottom panel shows anisotropic pendulum ($\delta = 0.01\,\mathrm{rad}^2/\mathrm{s}^2$) with rotating mount ($\Omega = 10\,\mathrm{rad\,s}^{-1}$). Pendulum length and initial conditions are the same as for data in figure 2.

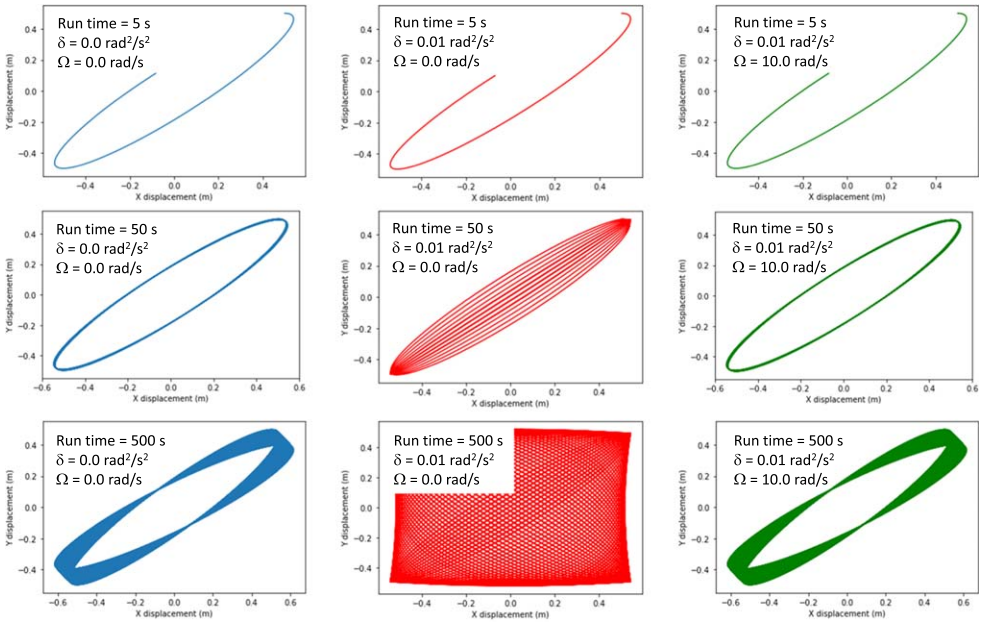

Figure 4. Trajectories of 2D pendulum (x displacement versus y displacement) in nonlinear regime calculated using odeint. Left panel shows isotropic pendulum ($\delta = 0\ \mathrm{rad}^2/\mathrm{s}^2$) with stationary mount ($\Omega = 0\ \mathrm{rad\ s}^{-1}$) at times 5 s (top), 50 s (middle) and 500 s (bottom). The middle panel shows an anisotropic pendulum ($\delta = 0.01\ \mathrm{rad}^2/\mathrm{s}^2$) with stationary mount ($\Omega = 0\ \mathrm{rad\ s}^{-1}$) at times 5 s (top), 50 s (middle) and 500 s (bottom). The right panel shows an anisotropic pendulum ($\delta = 0.01\ \mathrm{rad}^2/\mathrm{s}^2$) with rotating mount ($\Omega = 10\ \mathrm{rad\ s}^{-1}$) at times 5 s (top), 50 s (middle) and 500 s (bottom). For all these calculations the pendulum length was set to 10 m, with initial conditions of $x = 0.5$ m, $v_x = 0.2\ \mathrm{m\ s}^{-1}$, $y = 0.5$ m, and $v_y = 0.0\ \mathrm{m\ s}^{-1}$.

track the natural precession for any appreciable period of time. Finally, the evolution of motion for the case of the rotating anisotropic system is identical to that of the isotropic system in the left-hand panel and the natural precession is again clearly observable. In both cases the direction of the precession follows that of the elliptical motion as expected, clockwise in the case of the example shown in figure 4.

The precession of the vertices of the motion as a function of time for both the isotopic mount and rotating anisotropic mount pendulums, for two different initial conditions and pendulum parameters in both cases (including differing directions of pendulum motion and hence vertex precession, clockwise and counterclockwise), is shown in the supplemental material (figure SI-7), and the slope of the linear best fits are compared with the expected value from the equation $3\omega(ab)/8l^2$. As noted previously, we utilise initial conditions with relatively small displacement and velocity values which allow comparison with this equation. Excellent agreement is found with this theoretical prediction and again the rotation of the anisotropic mount means that the orbit pattern of the isotropic mount is recovered. These simulations all show strong evidence that the effects of the anisotropy in the system are effectively suppressed by the rotation of the mount and that the swing pattern of an isotropic 2D pendulum is recovered.

The angular rotation frequency of the mount is clearly an important parameter. The simulation results shown in figures 2–4 were based on the mount being rotated at angular

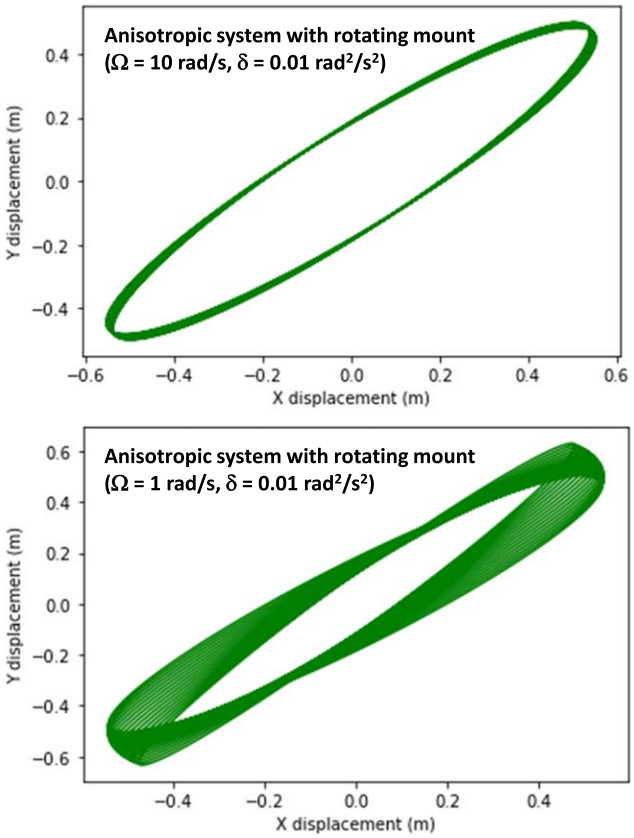

Figure 5. Trajectories of 2D pendulum (x displacement versus y displacement) in nonlinear regime calculated using odeint. Top image shows an anisotropic pendulum ($\delta = 0.01\ \mathrm{rad}^2/\mathrm{s}^2$) with a rotating mount ($\Omega = 10\ \mathrm{rad\ s}^{-1}$) after 100 s while the bottom image shows the same system with $\Omega = 1\ \mathrm{rad\ s}^{-1}$ after 100 s, where the effects of anisotropy are clearly evident. For all these calculations the pendulum length was set to 10 m, with initial conditions of $x = 0.5$ m, $v_x = 0.2\ \mathrm{m\ s}^{-1}$, $y = 0.5$ m, and $v_y = 0.0\ \mathrm{m\ s}^{-1}$.

frequency equal to approximately ten times that of the mean pendulum swing frequency in the PA frame, ω. Similar results are obtained for larger values of the mount rotation frequency relative to ω (i.e. the ratio Ω/ω). For values of the ratio Ω/ω close to (or less than) one, the motion of the rotating anisotropic mount pendulum no longer shows a pattern of motion whereby the effects of mount anisotropy are effectively suppressed, as case be seen in figure 5. In the range $1 < \Omega/\omega < 3$ the pattern of motion can depend on the exact value of the ratio Ω/ω. As noted previously, the effective rotation frequency of the mount is actually 2Ω.

3.3. Examples of possible extensions for open-ended studies

3.3.1. Angular momentum (non-)conservation. The rotation of the mount could in practice be achieved by a driving torque, the details of which are not explored in this work. In the case of a driven anisotropic system neither the energy nor the z-component of the angular momentum will be constant, so the motion of the anisotropic system with rotating mount will

not be identical to that of the isotropic system. Since the generalisation to the case of a system with anisotropy, as in equations (1), will depend on the specific physical origin of the anisotropy, which can vary depending on the design of the mount, the energy of the system will also depend on the physical origin of the asymmetry. We show the variation of the z-component of the angular momentum for the stationary isotropic mount system and the rotating anisotropic system in the supplemental material (figure SI-8), so that the small differences between the two systems may be appreciated (a fluctuation of $\sim$0.1% in the case of a rotating anisotropic mount, compared to variations two orders of magnitude smaller or more for the isotropic mount, which are due to intrinsic accumulation of errors in the numerical computations).

3.4. Random variations in PA orientation

We have explored the effects of random variations in the orientation of the PA of an anisotropic system, which is another situation in which an averaging out of the effects of the anisotropy of the pendulum system would be expected and which is quite different to that of the steady rotation discussed above. We have compared this situation to both a stationary anisotropic system and an anisotropic system whose mount is rotating at a constant angular rate. These data are shown in the supplemental material (figure SI-9) where the top, middle and bottom panels show the evolution of trajectories over a period of 400 s for a stationary anisotropic system, for an anisotropic system with random axis orientation variations, and for a steadily rotating anisotropic system, respectively. Some further comments on this approach and the details of the calculations are also provided in the supplemental material. It is apparent from these data that some suppression of the effects of mount anisotropy are also observed in the case of a random variation of the PA orientation, but that the clear and steadily precessing elliptical trajectory seen for a steadily rotating mount is not recovered, indicating that full suppression of mount anisotropy is not achieved (naturally run to run variations are seen for the simulation with random axis orientation variations).

4. Conclusion

We have presented a computational study of the effects of spinning the mount of an anisotropic pendulum during the pendulum motion. It is seen that in both the small angle, linear approximation, as well as in the case of motion beyond the small angle approximation, the effect of spinning the pendulum mount is to effectively suppress the effects of the anisotropy of the system, stabilising the motion of the pendulum and leading to a behaviour identical to that of an isotropic pendulum system, in agreement with the limited experimental evidence in the literature [2, 3]. We have also studied the effects of the anisotropy of the pendulum upon the swing evolution in the presence of random variations in the orientation of the PA of the mount and see that some suppression of the anisotropy is also observed in this situation.

The suppression of the effects of anisotropy in a pendulum by use of a rotating mount was initially suggested by Léon Foucault, based on his observations of the vibrations of a rod clamped in a lathe. It does not appear to ever have been used in practice, likely due to the difficulties in implementing it, even for an experimentalist as skilled as Foucault undoubtedly was. However, the use of computational techniques provides modern students with an alternative avenue of exploration and allows confirmation of Foucault's original observations and hypothesis and provides an interesting avenue for students to directly engage in a challenging and meaningful way with this historically important experiment.

Acknowledgments

We are very grateful to Dr Paul van Kampen, of the School of Physical Sciences in Dublin City University, for helpful discussions and very insightful feedback on the manuscript.

Data availability statement

All data that support the findings of this study are included within the article (and any supplementary files).

ORCID iDs

E McGlynn https://orcid.org/0000-0002-3412-9035

References

[1] Nelson R A and Olsson M G 1998 The pendulum—rich physics from a simple system *Am. J. Phys.* **54** 112
[2] Tobin W and Pippard B 1994 Foucault, his pendulum and the rotation of the earth *Interdiscip. Sci. Rev.* **19** 326–37
[3] Tobin W 2003 *The Life and Science of Léon Foucault—The Man Who Proved the Earth Rotates* (Cambridge University Press)
[4] Pippard A B 1988 The parametrically maintained foucault pendulum and its perturbations *Proc. R. Soc.*A **420** 81–91
[5] Longden A C 1919 On the irregularities of motion of the foucault pendulum *Phys. Rev.* **13** 241
[6] Dasannacharya B 1938 LII. The development of the minor axis in a Foucault's pendulum *London, Edinburgh Dublin Phil. Mag. J. Sci.* **25** 601–22
[7] Dasannacharya B and Hejmadi D 1937 VI. Rotation of the earth and Foucault's pendulums of short lengths *London, Edinburgh Dublin Phil. Mag. J. Sci.* **23** 65–88
[8] Schulz-Dubois E O 1970 Foucault pendulum experiment by Kamerlingh Onnes and degenerate perturbation theory *Am. J. Phys.* **38** 173–88
[9] Crane H R 1981 Short foucault pendulum: a way to eliminate the precession due to ellipticity *Am. J. Phys.* **49** 1004–6
[10] Schumacher R A and Tarbet B 2020 A short Foucault pendulum free of ellipsoidal precession arXiv:0902.1829
[11] Foucault L 1851 Démonstration physique du mouvement de rotation de la terre au moyen du pendule *C. R. Acad. Sci.* **32** 135–8
[12] Deakin M A B 2013 The ellipsing pendulum *Int. J. Math. Educ. Sci. Technol.* **44** 745–52
[13] Flannery W 2023 A revolution in physics education was forecast in 1989, why hasn't it happened? What will it take? *Am. J. Phys.* **91** 256
[14] De Jong M L 1992 Chaos and the simple pendulum *Phys. Teach.* **30** 115–21
[15] Guckenheimer J 1980 Dynamics of the Van der Pol equation *IEEE Trans. Circuits Syst.* **27** 983–9
[16] Choubey C K and Paul S K 2020 Implementation of chaotic oscillator by designing a simple Chua's diode using a single VDTA *AEU—Int. J. Electron. Commun.* **124** 153360
[17] Volos C 2023 Dynamical analysis of a memristive Chua's oscillator circuit *Electronics* **12** 4734
[18] Kubo R 1962 A stochastic theory of line shape and relaxation *Fluctuation, Relaxation, and Resonance in Magnetic Systems: Scottish Universities' Summer School 1961* ed D Ter Haar (Oliver & Boyd) pp 23–68
[19] Levitt M H 2015 *Spin Dynamics: Basics of Nuclear Magnetic Resonance* 2nd edn (Wiley)
[20] Keeler J 2006 *Understanding NMR Spectroscopy* 2nd edn (Wiley)
[21] Kirillov O N 2011 Brouwer's problem on a heavy particle in a rotating vessel: wave propagation, ion traps, and rotor dynamics *Phys. Lett.* **375** 1653–60
[22] Kirillov O N and Levi M 2016 Rotating saddle trap as Foucault's pendulum *Am. J. Phys.* **84** 26–31
[23] Stephenson A 1908 On induced stability *London, Edinburgh Dublin Phil. Mag. J. Sci.* **15** 233–6

[24] Veselić K 1995 On the stability of rotating systems *ZAMM—J. Appl. Math. Mech./Z. Angew. Math. Mech.* **75** 325–8
[25] Thompson R I, Harmon T J and Ball M G 2011 The rotating-saddle trap: a mechanical analogy to RF-electric-quadrupole ion trapping? *Can. J. Phys.* **80** 1433–48
[26] Olsson M G 1981 Spherical pendulum revisited *Am. J. Phys.* **49** 531–4